

Research Paper

Natural Convection Flow in Semi-Trapezoidal Porous Enclosure Filled with Alumina-Water Nanofluid Using Tiwari and Das' Nanofluid Model

Nallapati VEDAVATHI¹⁾, Kothuru VENKATADRI²⁾,
Syed FAZURUDDIN^{3),4)}*, G. Sankara Sekhar RAJU⁴⁾

¹⁾ *Department of Mathematics*
Koneru Lakshmaiah Education Foundation
Vaddeswaram, India

²⁾ *Department of Mathematics*
Indian Institute of Information Technology
Sri City, Andhra Pradesh, India

³⁾ *Department of Mathematics*
Sreenivasa Institute of Technology and Management Studies
Chittoor, Andhra Pradesh, India

⁴⁾ *Department of Mathematics*
JNTUA College of Engineering
Pulivendula, Andhra Pradesh, India

*Corresponding Author e-mail: fazuruddinsyed@gmail.com

Nowadays, optimal parameters are necessary for heat transfer enhancement in different practical applications. A numerical simulation of natural convection in a semi-trapezoidal enclosure embedded with porous medium is presented. Stream function and temperature using the Darcy–Boussinesq approximation and Tiwari and Das' nanofluid model with new more realistic empirical correlations for the physical properties of the nanofluids are formulated. The developed partial differential equations are employed with the help of the stream function approach. The in-house developed computational MATLAB code is validated with the previously published work. The impact of a wide range of governing parameters on fluid flow patterns and temperature gradient variations is presented. The thermal Rayleigh number (Ra) can be a control key parameter for heat and convective flow. Thermal dispersion effects are also examined in this study. An increase in the Rayleigh number leads to an increase in heat transfer, where one can find a reduction of convective heat transfer with ϕ .

Keywords: natural convection; laminar flow; porous medium; nanofluid; semi-trapezoidal enclosure.

1. INTRODUCTION

Heat transport and fluid flow in an enclosure embedded with a porous medium are well-known natural phenomena and they have attracted researchers' attention due to their practical applications, which include solar absorber collector systems [1], foam processing [2], geothermal power [3], borehole heat exchangers [4], wavy surface hybrid heat transfer devices [5, 6], biomechanics [7], gastric bio-transport [8], bio-fuel cells [9] and industrial filtration [10]. Engineers have, therefore, extensively examined natural convection flows in enclosures filled with porous media and also various modeling approaches.

According to [15] it is "a porous enclosure heated from the inner circular side and cooled from the outer circular side" to study the free convective flow of magnetic nanofluid with an impact of Brownian motion and thermal conductivity using the control volume finite element method (CVFEM). The study on several parameters such as Darcy, Hartmann, Rayleigh numbers and angle of magnetic field parameter identified a direct relationship between convective flow and Darcy number and Rayleigh number, and an inverse relationship was found between an inclination angle and Hartmann number. SIVASANKARAN *et al.* [16] adopted a non-Darcy porous model for the analysis of convective flow and heat expansion of Casson fluid within a porous square enclosure with sinusoidal thermal radiation. Using the SIMPLE algorithm, the obtained results show that the high values of Casson parameter under radiation generate a thermal stratification phenomenon. Deterioration of heat transport for the rising values of radiation parameter and improvement of heat transfer for the increasing values of Casson parameter were observed.

A new type of nanofluids is nano encapsulated phase change material (NEPCM), where nanoparticles are made of a shell and a core. SEYYEDI *et al.* [17] examined the characteristics of free convection flow, entropy generation, and heat transfer of NEPCMs in an enclosure filled with a porous medium. HASHEMI-TILEHNOEE *et al.* [18] used the finite volume method (FVM) conjugated with a non-dimensionalization scheme using ANSYS Fluent to study the natural convection analysis conjugated with entropy generation analysis in an incinerator-shaped permeable enclosure loaded with $\text{Al}_2\text{O}_3\text{-H}_2\text{O}$ nanofluid subjected to the magnetic field with a rectangular wavy heater block positioned on the bottom of the cavity wall. The bottom and top horizontal walls were adiabatic; the inclined and vertical walls were considered to be cooled. RAIZAH *et al.* [19] considered three distinct thermal conditions including conducting solid, hot solid and cold solid particles within the E-shaped enclosure partially filled with a porous medium to analyze the flow behavior and heat transfer of nanofluid. The results revealed that the fluid flow and heat transfer were increased within the enclosure for the case of the hot solid particles.

The encapsulation technique of phase change materials in the nano dimension is an innovative approach to improve the heat transfer capability and solve the issues of corrosion during the melting process. This new type of nanoparticle was suspended in base fluids call NEPCMs, nano encapsulated phase change materials [20]. SEYYEDI *et al.* [20] analyzed the impacts of pertinent parameters on the free convection and entropy generation in an elliptical-shaped enclosure filled with NEPCMs by considering the effect of an inclined magnetic field.

Heat transfer, free convective flow and entropy generation of water, Al_2O_3 -water, and NEPCM diluted in water as NEPCM-water suspension in a hot enclosure were examined by HASHEMI-TILEHNOEE *et al.* [21]. The enclosure was a square porous cavity heated from below, and the remaining walls were thermally insulated. The cavity was cooled by four cooling channels with three different configurations. SEYYEDI [22] used the CVFEM to examine the heat transfer behavior of a cardioid-shaped porous enclosure. In addition, the flow and heat transport were studied in four modes of the cardioid called in the investigation cases A, B, C, and D.

SUN and POP [23] investigated numerically the steady-state free convection heat transfer behavior of nanofluids inside a right-angle triangular enclosure filled with a porous medium. The governing equations were obtained based on Darcy's law and the nanofluid model proposed by TIWARI and DAS [38]. LIU *et al.* [24] studied free convection and entropy generation of water- Al_2O_3 nanofluid inside an inclined enclosure formed by connecting two inclined triangular cavities under a horizontal magnetic field. In this enclosure, half of the right walls of the cavity were hot and the remaining walls were adiabatic. As a result, entropy generation decreased and Bejan number increased for a high inclination angle.

The present study is motivated by the need to determine the detailed flow and temperature characteristics as well as the local and average Nusselt numbers. To the best knowledge of the authors, no study which considers this problem has yet been reported in the literature. As such, the focus of this paper is to examine the effects of pertinent parameters such as the Rayleigh number for a porous medium, and the solid volume fraction parameter of nanofluids.

2. MATHEMATICAL MODELING

Consider the steady free convection flow and heat transfer in a porous semi-trapezoidal enclosure filled with a Cu-water-based nanofluid. A schematic diagram of the problem under investigation is shown in Fig. 1. It is assumed that nanoparticles are suspended in the nanofluid using either surfactant or surface charge technology. This prevents nanoparticles from agglomeration and deposition on the porous matrix [11–14]. Here x and y are the coordinates of the

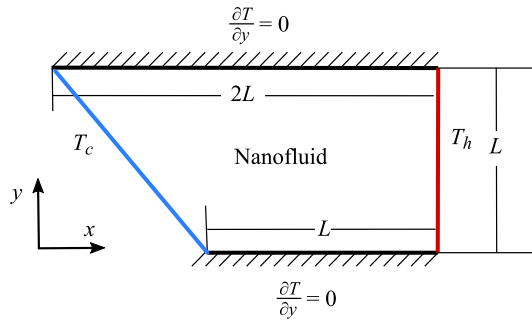


FIG. 1. Schematic diagram of the domain.

Cartesian geometry, and L is the length of the semi-trapezoidal enclosure. It is assumed that the right side is heated and kept at a high temperature T_h . The Darcy–Boussinesq approximation is employed. Under these assumptions and using the model of the nanofluid proposed by TIWARI and DAS [38], the equations governing this problem are

continuity:

$$(2.1) \quad \nabla \mathbf{V} = 0,$$

momentum [23, 39]:

$$(2.2) \quad \nabla p = -\frac{\mu_{mnf}}{K} \mathbf{V} - (\rho\beta)_{nf} (T - T_c) g,$$

energy:

$$(2.3) \quad (\mathbf{V} \cdot \nabla) T = \frac{k_{mnf}}{(\rho C_p)_{nf}} (\nabla^2 T) - \frac{1}{(\rho C_p)_{nf}} (\nabla \cdot q_r),$$

where \mathbf{V} denotes the Darcian velocity vector, K denotes porous medium permeability, g denotes the gravitation acceleration vector, μ denotes the dynamic viscosity, p denotes density, k denotes thermal conductivity, C_p represents specific heat at a fixed pressure, and β denotes thermal expansion coefficient.

The nanofluid physical properties: viscosity (μ_{nf}), heat capacitance $(\rho C_p)_{nf}$, buoyancy coefficient $(\rho\beta)_{nf}$, and thermal conductivity (k_{nf}) are:

$$(2.4) \quad \begin{aligned} \mu_{nf} &= \frac{\mu_f}{(1 - \phi)^{2.5}}, \\ (\rho C_p)_{nf} &= (1 - \phi) (\rho C_p)_f + \phi (\rho C_p)_s, \\ (\rho\beta)_{nf} &= (1 - \phi) (\rho\beta)_f + \phi (\rho\beta)_s, \\ \frac{k_{nf}}{k_f} &= \frac{k_s + 2k_f - 2\phi(k_f - k_s)}{k_s + 2k_f + \phi(k_f - k_s)}, \end{aligned}$$

where ϕ denotes the uniform concentration of the nanoparticles in the enclosure and indices nf, f , and s indicate nanofluid, fluid, and nanoparticle, respectively. The nanofluid dynamic viscosity (μ_{nf}) can be approximated in terms of the viscosity of the base fluid (μ_f) consisting of a dilute suspension of the fine spherical particles stated in [25]. It is worth mentioning that expression (2.4) is restricted to spherical nanoparticles, as it does not account for other shapes of nanoparticles. The thermophysical properties of the nanofluid and solid structure of the porous medium are given in Table 1. These thermophysical properties of the nanofluids were also used by KHANAFAER *et al.* [26], OZTOP and ABU-NADA [27], ABU-NADA and OZTOP [28], and MUTHAMILSELVAN *et al.* [29]. Further, it should be noted that for $k_s \gg k_f$ it results in the following limitation:

$$(2.5) \quad k_{nf} \approx k_f \frac{1 + 2\phi}{1 - \phi}$$

which limits the present study to the value of k_{nf} given by this relation.

Table 1. Thermophysical properties of fluid and copper (Cu) nanoparticles.

Physical properties	Base fluid (water)	Cu
C_p [J/(kg · K)]	4179	385
ρ [kg/m ³]	997.1	2700
k [W/(m · K)]	0.613	205
$\alpha \times 10^{-7}$ [m ² /s]	1.47	846.4
$\beta \times 10^{-5}$ [K ⁻¹]	21	2.22

On the other hand, we have (see [30]):

$$(2.6) \quad (\rho C_p)_m = \varepsilon (\rho C_p)_f + (1 - \varepsilon) (\rho C_p)_s, \quad k_m = \varepsilon k_f + (1 - \varepsilon) k_s,$$

and using the relations (2.4) and (2.6), the physical properties (heat capacitance, thermal conductivity and thermal diffusivity) of the nanofluid saturated porous medium are given by:

$$(2.7) \quad (\rho C_p)_{mnf} = \varepsilon (\rho C_p)_{nf} + (1 - \varepsilon) (\rho C_p)_s = (\rho C_p)_m \left[1 - \varepsilon \phi \frac{(\rho C_p)_f - (\rho C_p)_s}{(\rho C_p)_m} \right],$$

$$k_{mnf} = \varepsilon k_{nf} + (1 - \varepsilon) k_s = k_m \left\{ 1 - \frac{3\varepsilon \phi k_f (k_f - k_s)}{k_m [k_s + 2k_f + \phi(k_f - k_s)]} \right\},$$

$$\alpha_{mnf} = \frac{k_{mnf}}{(\rho C_p)_{nf}},$$

where ε is the porosity of the porous medium, α is the thermal diffusivity, and the subscripts mnf, s and m represent the nanofluid saturated porous medium,

solid matrix of the porous medium and clear fluid saturated porous medium, respectively. The enhancement of the thermal conductivity given in Eq. (2.7) is in agreement with the enhancement reported by YU *et al.* [31] for a common porous medium material saturated by a water base nanofluid:

$$q_r = (q_{rx}, q_{ry}, 0), \quad q_{rx} = -\frac{4\sigma}{3k^*} \frac{\partial T^4}{\partial x}, \quad q_{ry} = -\frac{4\sigma}{3k^*} \frac{\partial T^4}{\partial y}.$$

With the help of the Taylor series, we expand T^4 in terms of the low inclined wall temperature T_c and ignore higher-order terms, leading to:

$$T^4 \approx 4TT_c^3 - 3T_c^4.$$

With the help of the above, the radiative flux components are reduced to:

$$q_{rx} = -\frac{4\sigma T_c^3}{3k^*} \frac{\partial T}{\partial x}, \quad q_{ry} = -\frac{4\sigma T_c^3}{3k^*} \frac{\partial T}{\partial y}.$$

Equations (2.1)–(2.3) can be written in Cartesian coordinates as:

$$(2.8) \quad \frac{\partial u}{\partial x} + \frac{\partial v}{\partial y} = 0,$$

$$(2.9) \quad \frac{\mu_{mnf}}{K} \left(\frac{\partial u}{\partial y} - \frac{\partial v}{\partial x} \right) = -g(\rho\beta)_{nf} \frac{\partial T}{\partial x},$$

$$(2.10) \quad u \frac{\partial T}{\partial x} + v \frac{\partial T}{\partial y} = \alpha_{mnf} \left(\frac{\partial^2 T}{\partial x^2} + \frac{\partial^2 T}{\partial y^2} \right) + \frac{1}{(\rho c_p)_{nf}} \frac{16\sigma^* T_\infty^3}{3k^*} \left(\frac{\partial^2 T}{\partial x^2} + \frac{\partial^2 T}{\partial y^2} \right),$$

$$(2.11) \quad X = \frac{x}{L}, \quad Y = \frac{y}{L}, \quad U = \frac{uL}{\alpha_{mnf}},$$

$$V = vL/\alpha_{mnf}, \quad \theta = (T - T_c) / (T_h - T_c).$$

The fluid flow field introduced stream function ψ and it is defined as follows:

$$(2.12) \quad U = \frac{\partial \psi}{\partial y}, \quad V = -\frac{\partial \psi}{\partial x},$$

so, the governing equations are taken accounting for the stream function as follows:

$$(2.13) \quad \frac{\partial^2 \psi}{\partial x^2} + \frac{\partial^2 \psi}{\partial y^2} = -\text{Ra} \cdot H(\varphi) \frac{\partial \theta}{\partial x},$$

$$(2.14) \quad \frac{\partial \psi}{\partial Y} \frac{\partial \theta}{\partial X} - \frac{\partial \psi}{\partial X} \frac{\partial \theta}{\partial Y} = \left(1 + \frac{4}{3} \text{Rd} \right) \left(\frac{\partial^2 \theta}{\partial X^2} + \frac{\partial^2 \theta}{\partial Y^2} \right).$$

The dimensionless boundary conditions of domain of interest are:

$$\begin{aligned}
 (2.15) \quad & \psi = 0, \quad \theta = 0 \text{ on slant wall,} \\
 & \psi = 0, \quad \theta = 1 \text{ on right wall,} \\
 & \psi = 0, \quad \frac{\partial \theta}{\partial Y} = 0 \text{ on } Y = 0 \text{ and } Y = 1.
 \end{aligned}$$

Here,

$$Ra = gK (\rho\beta)_f (T_h - T_c) L / (\alpha_m \mu_f), \quad Rd = -\frac{4\sigma T_c^3}{kk^*},$$

and

$$H(\varphi) = \frac{\left[1 - \varphi + \varphi (\rho\beta)_p / (\rho\beta)_f\right] \left[1 - \varphi + \varphi (\rho C_p)_p / (\rho C_p)_f\right]}{1 - \frac{3\varepsilon\varphi k_f (k_f - k_p)}{k_m [k_p + 2k_f + \varphi(k_f - k_p)]}} (1 - \varphi)^{2.5}.$$

3. NUMERICAL METHOD

The partial differential Eqs. (2.13) and (2.14) of the present domain investigation and the corresponding boundary conditions (2.15) are employed with the help of the finite difference method (see [32–36]) with second-order accuracy. The stream function Poisson’s Eq. (2.14) is obtained from the Gauss-Seidel iterative method. The numerical methodology was coded in MATLAB. The developed computation algorithm is terminated when the stream function residual reaches below 10^{-8} . The in-house developed computational code is developed in MATLAB and verified against the work of [23] and [37]. Table 2 depicts the comparison of the mean Nusselt number Nu obtained for different Rayleigh numbers and the solid volume fraction from the other two references and it gives a good agreement.

Table 2. Comparison of the average Nusselt number in a porous triangular enclosure.

Ra	φ	Nu _{avg}		
		SUN and POP [23]	CHAMKHA and ISMAEL [37]	Present
500	0	9.66	9.52	9.63
1000	0	13.9	13.6	13.96
500	0.1	9.42	9.44	9.43

4. RESULTS AND DISCUSSION

A numerical investigation was performed for the boundary value problems from (2.13)–(2.15) on the following governing key parameters: Rayleigh number

($Ra = 10, 100, 500, 1000$), porosity parameter ($\varepsilon = 0.05, 0.5, 0.8, 1.2$), the solid volume fraction parameter of nanoparticles ($\phi = 0.04, 0.05$), and thermal radiation ($Rd = 0, 1.0, 1.2, 1.5, 2$). Impact-oriented particular outcomes were observed in the effects of these governing parameters for both the field of flow and temperature distribution of the nanofluid.

Rayleigh number is a very important parameter that has effects on heat transfer within a porous medium. Figure 2 depicts streamlines and isotherms for water-based Cu-nanofluid for various values of Ra with $Rd = 1, \phi = 0.05, \varepsilon = 0.5$ for the solid system of porous medium. Despite distinct values of Rayleigh number and structure of the porous medium, an anti-clockwise mono circulation of

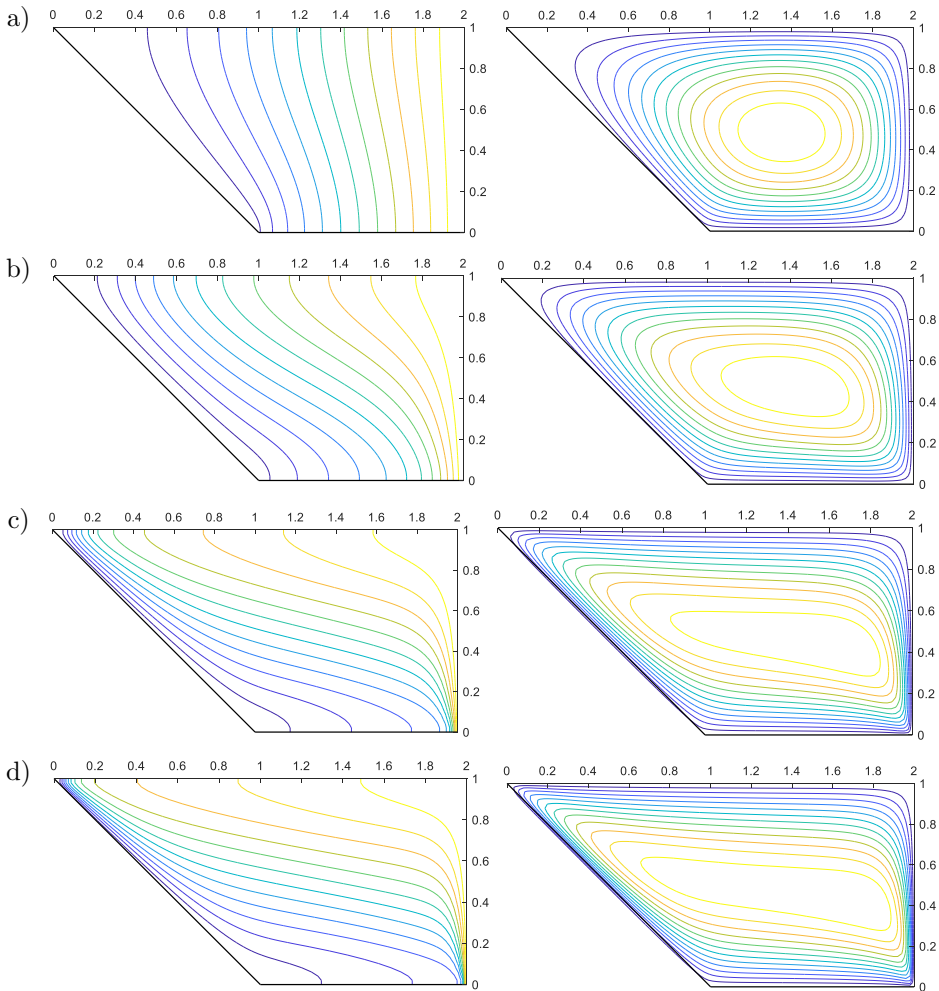


FIG. 2. Isotherms and streamlines contours for $Rd = 1, \phi = 0.05, \varepsilon = 0.5$:

a) $Ra = 10$; b) $Ra = 100$; c) $Ra = 500$; d) $Ra = 1000$.

the eddy was formed inside the cavity. When $Ra = 10$ (see Fig. 2a), a single circular eddy was generated inside the enclosure and the corresponding isotherms occupied the enclosure. When Ra values increased, the strength of viscous forces reduced and this led to the rise of buoyancy forces; accordingly, vortex strength inside the cavity was also enhanced. So, for $Ra = 100, 500, 1000$ (Figs. 2b–2d), the respective eddies inside the cavity were gradually enhanced and the shape of the eddy shifted from circular to elliptical. At $Ra = 1000$ (Fig. 2d), the maximum strength of the vortex was observed. When the Rayleigh number enhanced, the convective fluid cell was stronger, the convective circulation stretched towards the horizontal axis, and the thermal boundary layer along the cold wall was stronger. The former can be confirmed by the maximum absolute values of the stream function as the following:

$$|\psi|_{\max}^{Ra=10} = 0.29 < |\psi|_{\max}^{Ra=100} = 2.16 < |\psi|_{\max}^{Ra=500} = 6.75 < |\psi|_{\max}^{Ra=1000} = 10.78.$$

It is obvious that changes in free convective flows are directly related to the respective variations in the temperature field. At $Ra = 10$ (Fig. 2a), a weak heat transformation from the right hot wall to the left inclined cold wall was observed, and a considerable distribution of isotherms towards the cold wall was noticed. An increase in Rayleigh number (Ra) led to the rising strength of heat transformation along the inclined cold wall. At $Ra = 1000$ (Fig. 2d), the flow particles were boosted towards the cold wall and the thermal contours were steeper and more clustered near the cold wall. The thermal boundary layer formation was observed for greater values of the buoyancy forces. The thermal flume was stronger at the thermal Rayleigh number $Ra = 1000$, which is observed in Fig. 2d.

The porosity of the porous medium is another key factor that shows an impact on heat expansion inside the cavity. Figure 3 depicts streamlines and isotherms for distinct values of the porosity parameter ε at $\phi = 0.05$, with $Rd = 1, Ra = 1000$ for the solid system of porous field. Increasing values of ε led to insignificant changes in streamlines and isotherms. Such behavior can be confirmed by the maximum absolute values of the stream function:

$$|\psi|_{\max}^{\varepsilon=0.8} = 10.7789 < |\psi|_{\max}^{\varepsilon=0.5} = 10.7840 < |\psi|_{\max}^{\varepsilon=0.05} = 10.7856.$$

The solid volume fraction parameter (ϕ) is also another key parameter that helps us to analyze how nanoparticles show an impact in the heat transformation of nanofluids. Figure 4 depicts streamlines and isotherms for distinct values of ϕ , at $\varepsilon = 0.05, Ra = 1000$ for the solid system of porous field. When ϕ values were increased, attenuation in fluid flow was observed inside the cavity and did not show any impact on thermal expansion. When the concentration of nanoparticles inside the cavity increased the fluid flowed upward along

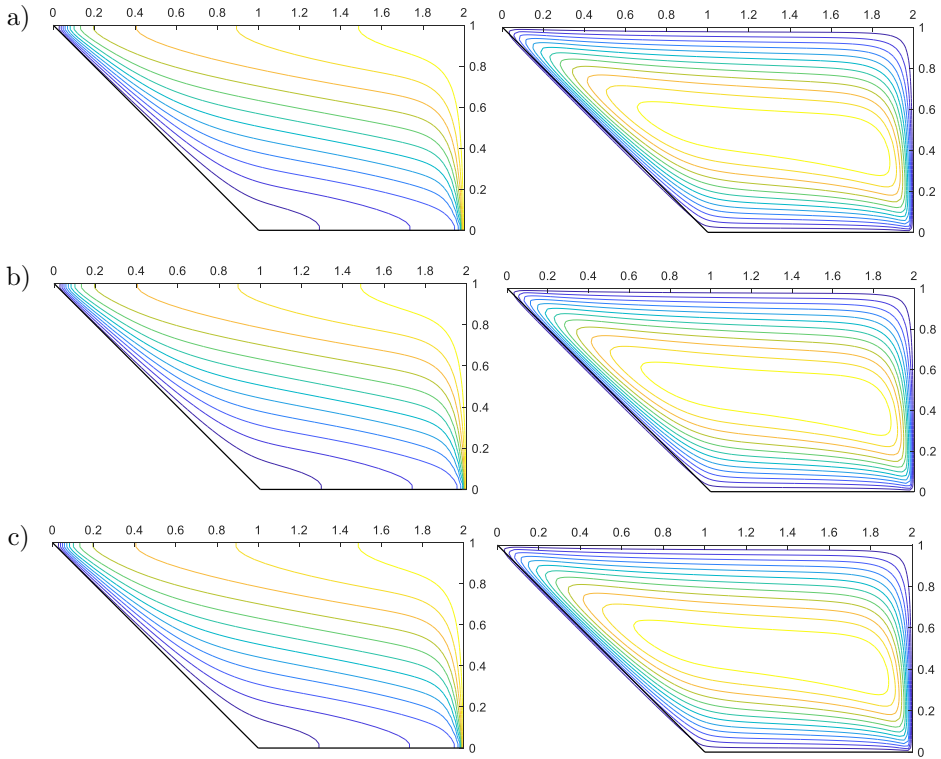


FIG. 3. Isotherms and streamlines contours for $Rd = 1$, $\phi = 0.05$, $Ra = 1000$:
 a) $\varepsilon = 0.05$; b) $\varepsilon = 0.5$; c) $\varepsilon = 0.8$.

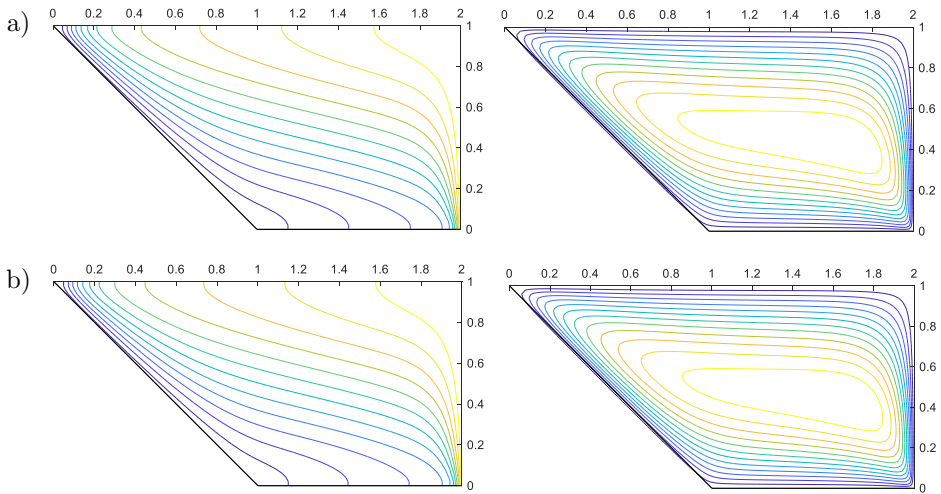


FIG. 4. Isotherms and streamlines contours for $Rd = 1$, $\varepsilon = 0.05$, $Ra = 1000$:
 a) $\phi = 0.04$; b) $\phi = 0.05$.

the right hot wall and downward along the left inclined cold wall. Such behavior can be confirmed by the maximum absolute values of the stream function $|\psi|_{\max}^{\phi=0.04} = 11.00 > |\psi|_{\max}^{\phi=0.05} = 10.78$. Figures 4 and 5 present the influence of thermal Rayleigh number, porosity and nanofluid volume fraction on the local Nusselt number, respectively. The heat transfer along the hot wall increased with Rayleigh number. In addition, insignificant heat distribution along the hot wall was observed for the impact of the porosity and nanofluid volume fraction. Figures 6 and 7 present the influence of the nanofluid volume fraction and thermal radiation parameter on the local Nusselt number of the isothermal hot wall, respectively. Significant changes are observed in heat transfer for the various values of Rd. In addition, it was observed that a more essential increment

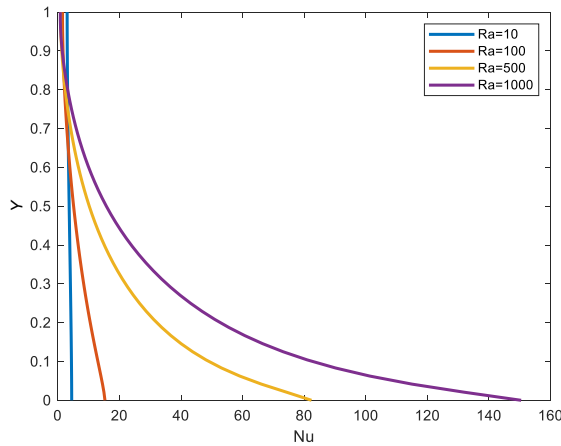


FIG. 5. Local Nusselt number variation of the hot wall with Ra for $\phi = 0.05$, $\varepsilon = 0.5$, Rd = 1.

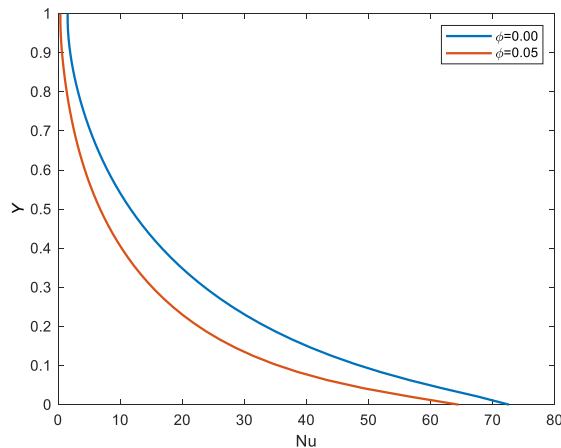


FIG. 6. Local Nusselt number variation of the hot wall with ϕ for Rd = 2, $\varepsilon = 0.05$, Ra = 1000.

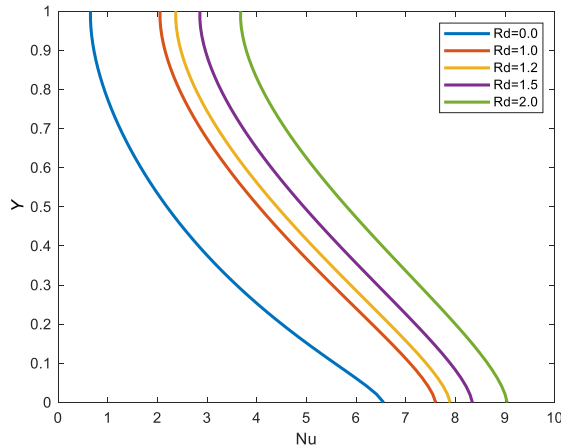


FIG. 7. Local Nusselt number variation of the hot wall with Rd for $\phi = 0.05$, $\varepsilon = 0.5$, $Ra = 100$.

of the Nusselt number with increase in ϕ and Rd occurred for the high thermal conductivity material of the solid matrix.

5. CONCLUSIONS

Natural convection in a semi-trapezoidal porous cavity with isothermal vertical and inclined walls, with adiabatic horizontal ones filled with a water-based nanofluid, was studied. Particular efforts focused on the effects of the thermal radiation, Rayleigh number, solid volume fraction parameter of nanoparticles, the porosity of the porous medium and solid matrix of the porous medium on temperature distribution, flow field, and Nusselt number. An insignificant heat distribution (local Nusselt number) was observed for the impact of the porosity parameter and nanofluid volume fraction. It was found that the local Nusselt number is an increasing function of the thermal Rayleigh number and thermal radiation parameter, and the thermal Rayleigh number (Ra) can be a control key parameter for heat and convective flow. In addition, thermal dispersion effects were examined in this study. An increase in the Rayleigh number led to an increase in heat transfer, where one can find a reduction of convective heat transfer with ϕ .

FUNDING

There was no funding source available for this research paper.

CONFLICT OF INTEREST

All the authors have no conflict of interest in publishing this article.

INFORMED CONSENT

Informed consent was obtained from all individual participants included in the study.

AUTHORSHIP CONTRIBUTION

All the authors contributed equally to this research paper.

ACKNOWLEDGMENTS

The authors are grateful to the reviewers for their comments improving the article.

REFERENCES

1. SINGH S., Experimental and numerical investigations of a single and double pass porous serpentine wavy wire mesh packed bed solar air heater, *Renewable Energy*, **145**: 1361–1387, 2020, doi: 10.1016/j.renene.2019.06.137.
2. DUKHAN N., Analysis of Brinkman-extended Darcy flow in porous media and experimental verification using metal foam, *ASME. Journal of Fluids Engineering*, **134**(7): 071201, 2012, doi: 10.1115/1.4005678.
3. BÉG O.A., MOTSA S.S., KADIR A., BÉG T.A., ISLAM M.N., Spectral quasilinear numerical simulation of micropolar convective wall plumes in high permeability porous media, *Journal of Engineering Thermophysics*, **25**: 576–599, 2016, doi: 10.1134/S1810232816040147.
4. CHOI W., OOKA R., Effect of natural convection on thermal response test conducted in saturated porous formation: Comparison of gravel-backfilled and cement-grouted borehole heat exchangers, *Renewable Energy*, **96**(Part A): 891–903, 2016, doi: 10.1016/j.renene.2016.05.040.
5. BÉG O.A., MOTSA S.S., BÉG T.A., ABBAS A.J., KADIR A., SOHAIL A., Numerical study of nonlinear heat transfer from a wavy surface to a high permeability medium with pseudo-spectral and smoothed particle methods, *International Journal of Applied and Computational Mathematics*, **3**: 3593–3613, 2017, doi: 10.1007/s40819-017-0318-4.
6. BELABID J., Impact of wall waviness on the convection patterns inside a horizontal porous annulus, *ASME. Journal of Fluids Engineering*, **142**(7): 071304, 2020, doi: 10.1115/1.4406481.
7. VAFAI K. [Ed], *Porous Media: Applications in Biological Systems and Biotechnology*, CRC Press, 1st ed., Boca Raton, Florida, 2010.

8. TRIPATHI D., BÉG O.A., A numerical study of oscillating peristaltic flow of generalized Maxwell viscoelastic fluids through a porous medium, *Transport in Porous Media*, **95**: 337–348, 2012, doi: 10.1007/s11242-012-0046-5.
9. BÉG O.A., PRASAD V.R., VASU B., Numerical study of mixed bioconvection in porous media saturated with nanofluid and containing oxytactic micro-organisms, *Journal of Mechanics Medicine and Biology*, **13**(4): 1350067, 2013, doi: 10.1142/S021951941350067X.
10. CALTAGIRONE J.P., Thermoconvective instabilities in a porous medium bounded by two concentric horizontal cylinders, *Journal of Fluid Mechanics*, **76**(2): 337–362, 1976, doi: 10.1017/S0022112076000669.
11. KUZNETSOV A.V., NIELD D.A., The onset of double-diffusive nanofluid convection in a layer of a saturated porous medium, *Transport in Porous Media*, **85**: 941–951, 2010, doi: 10.1007/s11242-010-9600-1.
12. KUZNETSOV A.V., NIELD D.A., The Cheng–Minkowycz problem for natural convective boundary layer flow in a porous medium saturated by a nanofluid: a revised model, *International Journal of Heat and Mass Transfer*, **65**: 682–685, 2013, doi: 10.1016/j.ijheatmasstransfer.2013.06.054.
13. NIELD D.A., KUZNETSOV A.V., The Cheng–Minkowycz problem for natural convective boundary-layer flow in a porous medium saturated by a nanofluid, *International Journal of Heat and Mass Transfer*, **52**(25–26): 5792–5795, 2009, doi: 10.1016/j.ijheatmasstransfer.2009.07.024.
14. NIELD D.A., KUZNETSOV A.V., Thermal instability in a porous medium layer saturated by a nanofluid: a revised model, *International Journal of Heat and Mass Transfer*, **68**: 211–214, 2014, doi: 10.1016/j.ijheatmasstransfer.2013.09.026.
15. DOGONCHI A.S., SEYYEDI S.M., HASHEMI-TILEHNOEE M., CHAMKHA A.J., GANJI D.D., Investigation of natural convection of magnetic nanofluid in an enclosure with a porous medium considering Brownian motion, *Case Studies in Thermal Engineering*, **14**: 100502, 2019, doi: 10.1016/j.csite.2019.100502.
16. SIVASANKARAN S., BHUVANESWARI M., ALZHRANI A.K., Numerical simulation on convection of non-Newtonian fluid in a porous enclosure with non-uniform heating and thermal radiation, *Alexandria Engineering Journal*, **59**: 3315–3323, 2020, doi: 10.1016/j.aej.2020.04.045.
17. SEYYEDI S.M., HASHEMI-TILEHNOEE M., SHARIFPUR M., Impact of fusion temperature on hydrothermal features of flow within an annulus loaded with nanoencapsulated phase change materials (NEPCMs) during natural convection process, *Mathematical Problems in Engineering*, **2021**: Article ID 4276894, 2021, doi: 10.1155/2021/4276894.
18. HASHEMI-TILEHNOEE M., DOGONCHI, A.S., SEYYEDI S.M., CHAMKHA A.J., GANJI D.D., Magnetohydrodynamic natural convection and entropy generation analyses inside a nanofluid-filled incinerator-shaped porous cavity with wavy heater block, *Journal of Thermal Analysis and Calorimetry*, **141**(5): 2033–2045, 2020, doi: 10.1007/s10973-019-09220-6.
19. RAIZAH Z.A.S., AHMED S.E., ALY A.M., ISPH simulations of natural convection flow in E-enclosure filled with a nanofluid including homogeneous/heterogeneous porous media and solid particles, *International Journal of Heat and Mass Transfer*, **160**: 120153, 2020, doi: 10.1016/j.ijheatmasstransfer.2020.120153.

20. SEYYEDI S.M., HASHEMI-TILEHNOEE M., SHARIFPUR M., Effect of inclined magnetic field on the entropy generation in an annulus filled with NEPCM suspension, *Mathematical Problems in Engineering*, **2021**: Article ID 8103300, 2021, doi: 10.1155/2021/8103300.
21. HASHEMI-TILEHNOEE M., DOGONCHI A.S., SEYYEDI S.M., SHARIFPUR M., Magneto-fluid dynamic and second law analysis in a hot porous cavity filled by nanofluid and nano-encapsulated phase change material suspension with different layout of cooling channels, *Journal of Energy Storage*, **31**: 101720, 2020, doi: 10.1016/j.est.2020.101720.
22. SEYYEDI S.M., On the entropy generation for a porous enclosure subject to a magnetic field: different orientations of cardioid geometry, *International Communications in Heat and Mass Transfer*, **116**: 104712, 2020, doi: 10.1016/j.icheatmasstransfer.2020.104712.
23. SUN Q., POP I., Free convection in a triangle cavity filled with a porous medium saturated with nanofluids with flush mounted heater on the wall, *International Journal of Thermal Sciences*, **50**(11): 2141–2153, 2011, doi: 10.1016/j.ijthermalsci.2011.06.005.
24. LIU W., SHAHSAVAR A., BARZINJY A.A., AL-RASHED A.A.A.A., AFRAND M., Natural convection and entropy generation of a nanofluid in two connected inclined triangular enclosures under magnetic field effects, *International Communications in Heat and Mass Transfer*, **108**: 104309, 2019, doi: 10.1016/j.icheatmasstransfer.2019.104309.
25. BRINKMAN H.C., The viscosity of concentrated suspensions and solutions, *The Journal of Chemical Physics*, **20**(4): 571–581, 1952, doi: 10.1063/1.1700493.
26. KHANAFAER K., VAFAI K., LIGHTSTONE M., Buoyancy-driven heat transfer enhancement in a two-dimensional enclosure utilizing nanofluids, *International Journal of Heat and Mass Transfer*, **46**(19): 3639–3653, 2003, doi: 10.1016/S0017-9310(03)00156-X.
27. OZTOP H.F., ABU-NADA E., Numerical study of natural convection in partially heated rectangular enclosures filled with nanofluids, *International Journal of Heat and Fluid Flow*, **29**(5): 1326–1336, 2008, doi: 10.1016/j.ijheatfluidflow.2008.04.009.
28. ABU-NADA E., OZTOP H.F., Effects of inclination angle on natural convection in enclosures filled with Cu-water nanofluid, *International Journal of Heat and Fluid Flow*, **30**(4): 669–678, 2009, doi: 10.1016/j.ijheatfluidflow.2009.02.001.
29. MUTHAMILSELVAN M., KANDASWAMY P., LEE J., Heat transfer enhancement of copper-water nanofluids in a lid-driven enclosure, *Communications in Nonlinear Science and Numerical Simulation*, **15**: 1501–1510, 2010, doi: 10.1016/j.cnsns.2009.06.015.
30. NIELD D.A., BEJAN A., *Convection in Porous Media*, 4th ed., Springer, New York, 2013.
31. YU W., FRANCE D.M., ROUTBORT J.L., CHOI S.U.S., Review and comparison of nanofluid thermal conductivity and heat transfer enhancements, *Heat Transfer Engineering*, **29**(5): 432–460, 2008, doi: 10.1080/01457630701850851.
32. VENKATADRI K., BÉG O.A., RAJARAJESWARI P., RAMACHANDRA PRASAD V., SUBBARAO A., HIDAYATHULLA KHAN B.Md., Numerical simulation and energy flux vector visualization of radiative-convection heat transfer in a porous triangular enclosure, *Journal of Porous Media*, **23**(12): 1187–1199, 2020, doi: 10.1615/JPorMedia.2020033653.
33. BÉG O.A., VENKATADRI K., PRASAD V.R., BÉG T.A., KADIR A., LEONARD H.J., Numerical simulation of hydromagnetic Marangoni convection flow in a Darcian porous semiconductor melt enclosure with buoyancy and heat generation effects, *Materials Science and Engineering: B*, **261**: 114722, 2020, doi: 10.1016/j.mseb.2020.114722.

34. VENKATADRI K., BÉG O.A., RAJARAJESWARI P., RAMACHANDRA PRASAD V., Numerical simulation of thermal radiation influence on natural convection in a trapezoidal enclosure: Heat flow visualization through energy flux vectors, *International Journal of Mechanical Sciences*, **171**: 105391, 2020, doi: 10.1016/j.ijmecsci.2019.105391.
35. VENKATADRI K., ABDUL GAFFAR S., RAJARAJESWARI P., RAMACHANDRA PRASAD V., BÉG O.A., HIDAYATHULLA KHAN B.Md., Melting heat transfer analysis of electrically conducting nanofluid flow over an exponentially shrinking/stretching porous sheet with radiative heat flux under a magnetic field, *Heat Transfer*, **49**(8): 4281–4303, 2020, doi: 10.1002/htj.21827.
36. VENKATADRI K., ABDUL GAFFAR S., SURYANARAYANA REDDY M., RAMACHANDRA PRASAD V., HIDAYATHULLA KHAN B.Md., BEG O.A., Melting heat transfer on magnetohydrodynamics buoyancy convection in an enclosure: A numerical study, *Journal of Applied and Computational Mechanics*, **6**(1): 52–62, 2020, doi: 10.22055/JACM.2019.28761.1504.
37. CHAMKHA A.J., ISMAEL M.A., Conjugate heat transfer in a porous cavity filled with nanofluids and heated by a triangular thick wall, *International Journal of Thermal Sciences*, **67**: 135–151 2013, doi: 10.1016/j.ijthermalsci.2012.12.002.
38. TIWARI R.K., DAS M.K., Heat transfer augmentation in a two-sided lid-driven differentially heated square cavity utilizing nanofluids, *International Journal of Heat and Mass Transfer*, **50**(9–10): 2002–2018, 2007, doi: 10.1016/j.ijheatmasstransfer.2006.09.034.

Received November 19, 2020; accepted version August 12, 2022.



Copyright © 2022 The Author(s).

This is an open-access article distributed under the terms of the Creative Commons Attribution-ShareAlike 4.0 International (CC BY-SA 4.0 <https://creativecommons.org/licenses/by-sa/4.0/>) which permits use, distribution, and reproduction in any medium, provided that the article is properly cited. In any case of remix, adapt, or build upon the material, the modified material must be licensed under identical terms.